Addiction Biology

ORIGINAL ARTICLE

doi:10.1111/adb.12234

Abnormal white matter structural networks characterize heroin-dependent individuals: a network analysis

Ruibin Zhang[1]*†, Guihua Jiang[2]*, Junzhang Tian[2]*, Yingwei Qiu[2]*, Xue Wen[1], Andrew Zalesky[3], Meng Li[2], Xiaofen Ma[2], Junjing Wang[1], Shumei Li[2], Tianyue Wang[2], Changhong Li[1] & Ruiwang Huang[1]

Centre for the Study of Applied Psychology, Guangdong Key Laboratory of Mental Healthy and Cognitive Science of Guangdong Province, School of Psychology, South China Normal University, China[1], Department of Medical Imaging, Guangdong No. 2 Provincial People's Hospital, China[2] and Melbourne Neuropsychiatry Centre, University of Melbourne and Melbourne Health, Australia[3]

ABSTRACT

Neuroimaging studies suggested that drug addiction is linked to abnormal brain functional connectivity. However, little is known about the alteration of brain white matter (WM) connectivity in addictive drug users and nearly no study has been performed to examine the alterations of brain WM connectivity in heroin-dependent individuals (HDIs). Diffusion tensor imaging (DTI) offers a comprehensive technique to map the whole brain WM connectivity in vivo. In this study, we acquired DTI datasets from 20 HDIs and 18 healthy controls and constructed their brain WM structural networks using a deterministic fibre tracking approach. Using graph theoretical analysis, we explored the global and nodal topological parameters of brain network for both groups and adopted a network-based statistic (NBS) approach to assess between-group differences in inter-regional WM connections. Statistical analysis indicated the global efficiency and network strength were significantly increased, but the characteristic path length was significantly decreased in the HDIs compared with the controls. We also found that in the HDIs, the nodal efficiency was significantly increased in the left prefrontal cortex, bilateral orbital frontal cortices and left anterior cingulate gyrus. Moreover, the NBS analysis revealed that in the HDIs, the significant increased connections were located in the paralimbic, orbitofrontal, prefrontal and temporal regions. Our results may reflect the disruption of whole brain WM structural networks in the HDIs. Our findings suggest that mapping brain WM structural network may be helpful for better understanding the neuromechanism of heroin addiction.

Keywords Addiction, diffusion tensor imaging, graph theory, network-based statistic.

Correspondence to: Ruiwang Huang, Center for the Study of Applied Psychology, Key Laboratory of Mental Healthy and Cognitive Science of Guangdong Province, School of Psychology, South China Normal University, Guangzhou 510631, China. E-mail: ruiwang.huang@gmail.com

INTRODUCTION

Drug addiction, a major health problem in modern society, is characterized by the failure to resist one's impulses to obtain and to take certain types of addictive drugs in spite of serious negative consequences (Volkow & Li 2004; Holmes 2012). Out of all drug abuses, heroin addiction is a major threat to the public health and social security in China because of its devastating medical effects, its impact on criminal behaviours and its low rates of recovery but high rates of relapse (Tang *et al.* 2006). It was because of the negative impacts of heroin addiction that many studies try to uncover the mechanisms of addiction from different fields (Koob 2002; Levran *et al.* 2008; Goldstein & Volkow 2011). With the neuroimaging technology, a growing number of studies suggested aberrant brain functional connectivity on the basis of resting-state functional magnetic resonance imaging (fMRI) data (Ma *et al.* 2010) and task-state fMRI data acquired in different stimulus paradigms, such as

*Ruibin Zhang, Guihua Jiang, Junzhang Tian and Yingwei Qiu contributed equally to this work.
†Present address: Department of Psychology, The University of Hong Kong, Pokfulam, Hong Kong.

drug craving (Xiao *et al.* 2006; Li *et al.* 2012), decision making (Walter *et al.* 2014) and inhibitory control (Schmidt *et al.* 2013), in heroin-dependent individuals (HDIs). Given that aberrant functional connectivity may be a result of the pathology of brain white mater (WM) connectivity, the next logical step is to understand the underlying structural architecture of brain WM in HDIs.

Diffusion tensor imaging (DTI) is a non-invasive technique to detect human brain tissue microstructure and to assess distribution of axonal fibre bundles in vivo (Mori & Zhang 2006). Several previous studies (Supporting Information Table S1) have reported the alterations of brain WM patterns related to heroin addiction on the basis of diffusive metrics (e.g. fractional anisotropy, FA). For example, Liu *et al.* (2009) analysed DTI datasets from 16 HDIs and 16 controls and found significantly decreased FA in HDIs in the bilateral frontal sub-gyral, right precentral and left cingulate regions compared with controls. Li *et al.* (2013) revealed decreased FA value in brain WM of the bilateral frontal lobes, cingulate gyri, medial frontal gyri and right superior frontal gyrus in HDIs. Notably, although most of previous studies analysed the myelin axonal distribution according to the hypothesis of WM disruption or inter-regional 'dysconnection' (Volkow *et al.* 2013), nearly no study has directly investigated axonal connectivity in HDIs *per se*.

Growing number of studies (Hagmann *et al.* 2010; Griffa *et al.* 2013; He & Evans 2014) have adopted a network model to characterize human brain cortical-cortical WM connectivity and suggested that the integrity of brain connectivity can be tested at the macroscale or at the scale of brain axonal fibre bundles in drug patients. For example, Zalesky *et al.* (2012b) found that the impaired WM fibre connectivity existed in the fornix, splenium of corpus callosum and commissural fibres in long-term cannabis users. As the brain WM connectivity reflects the integration of brain WM structure, many studies (Fornito *et al.* 2012; Griffa *et al.* 2013) have used the topology of brain networks to infer the integrity of brain network organization in different types of neuropsychiatry patients. A previous study (Kim *et al.* 2011) acquired DTI data from 12 cannabis users, analysed their brain WM structural networks and suggested less efficient integrated and altered regional connectivity in their brain WM structural networks. We have also seen that several studies (Liu *et al.* 2009; Yuan *et al.* 2010; Jiang *et al.* 2013) reported aberrant brain functional connectivity and disrupted topological organization in HDIs based on the resting-state fMRI data. However, the heroin addiction-related changes of brain WM connectivity and topological organization of the brain WM structural networks are still unknown.

The aim of this study was to detect the topological changes of brain WM structural networks related to heroin addiction at a macroscale (i.e. at the scale of WM fibre bundles). In the calculations, we constructed whole brain WM structural networks for both the HDIs and healthy controls based on the DTI data, evaluated their network metrics using graph theory and determined between-group differences in network topological parameters. In addition, we also used a network-based statistic (NBS) approach (Zalesky *et al.* 2012a) to identify the disrupted WM structural connections in the HDIs.

MATERIALS AND METHODS

Subjects

We recruited 20 HDIs (18 males, two females; aged 26–50 years, age = 35.0 ± 6.3 years) from the Addiction Medicine Division of Guangdong No. 2 Provincial People's Hospital. Among them, four inhaled the vapour from heated heroin, while 16 used intravenous and vapour from heated heroin. These HDIs were screened using the Structured Clinical Interview for the Diagnostic and Statistical Manual of Mental Disorders, Fourth Edition to confirm the diagnosis of heroin dependence. Urine tests with a positive finding for heroin users were requested before enrolling in the treatment programme. According to a laboratory report and an interview conducted in the hospital, none of the controls or HDIs had a history of excessive alcohol consumption. All of the HDIs were under daily methadone maintenance treatment at the time of the study and were hospitalized for 6–7 days before the MRI scanning took place. None of them used heroin during their stay in the hospital as confirmed by the medical personnel responsible for their care (Supporting Information Table S2). In addition, we recruited 18 age- and gender-matched healthy subjects as the controls (16 males, two females; aged 23–45 years, age = 33.1 ± 7.2 years). Table 1 lists the demographic details of all the volunteers in this study. None of the HDIs and the controls had history of neurological illness or head injury, or was diagnosed with schizophrenia or an affective disorder, according to their past medical history. All of the subjects were right-handed according to their self-report. This study was approved by the Research Ethics Review Board of the Southern Medical University in Guangzhou of China. Informed written consent was obtained from each subject prior to the MRI scanning.

Data acquisition

All MR scans were performed on a 1.5T Philip MRI scanner (Philip, Amsterdam, the Netherlands) equipped with an 8-channel head coil. To diminish motion artefacts, we immobilized each individual's head with cushions inside the coil after the alignment during the scan. The parameters of DTI sequence, signal-to-noise ratio

Table 1 Demographics and clinical characteristics of in the heroin-dependent individuals (HDIs) and the healthy controls (HCs).

Characteristics	*HDIs* (n = *20)*	*HCs* (n = *18)*	P *value*
Gender (female/male)	2/18	2/16	0.6832[a]
Age (years) [range in years]	35.0 ± 6.3 [27–50]	33.1 ± 7.2 [23–45]	0.4017[b]
Education (years) [range in years]	10.5 ± 2.5 [9–15]	10.1 ± 3.4 [6–16]	0.6950[b]
Head motion			
Translation	1.01 ± 0.61	0.92 ± 0.58	0.41[b]
Rotation	0.006 ± 0.01	0.007 ± 0.01	0.75[b]
Nicotine (median, number of cigarette/day)	20 [0–60]	20 [0–40]	0.3231[b]
Heroin use (years) [range in years]	9.8 ± 5.5 [1.3–20]	—	—
Heroin dosage (g/day) [range in g/day]	3.7 ± 2.27 [2–8]	—	—
Dosage of methadone (mg/day)	31.5 ± 13.48 [20–60]	—	—

The duration of heroin usage means the period from the time of initial heroin use to the time of their seeking medical help.
[a]Fisher's exact test. [b]Two-sample *t*-test.

(SNR) estimation of DTI data and estimates of head motion are provided in the Supporting Information Appendix S1.

Data pre-processing

The effects of head motion and image distortion caused by eddy current were corrected by applying an affine alignment to register all other diffusion volumes to the original b_0 volume using the Functional Magnetic Resonance Imaging of the Brain Software Library (FSL 4.1: http://www.fmrib.ox.ac.uk/fsl). Rotation corrections were applied to the corresponding diffusion-sensitive gradient directions (Leemans & Jones 2009). The corrected DTI data were then processed using Trackvis (http://trackvis.org/) to draw whole brain streamline counts based on the fibre assignment by continuous tracking algorithm, a deterministic fibre tracking approach. Fibre tracking was stopped when FA <0.2 or the angle between the eigenvectors of two consecutive voxels was less than 45°.

Network construction

We first co-registered T1-weighted three-dimensional volume to the original b_0 volume resulting in the co-registered T1 volume for each individual using SPM8 (www.fil.ion.ucl.ac.uk/spm). The co-registered T1 volumes were then non-linearly transformed to the ICBM-152 T1-weighted template in the standard Montreal Neurological Institute (MNI) space. The inverse transformations were used to warp the automated anatomical labelling template with 90 regions (AAL-90) from the standard MNI space to the individual native DTI space using a nearest-neighbour interpolation approach. The names and the abbreviations for these 90 regions are listed in Supporting Information Table S3.

We used an abstract model of brain network to represent the brain systems at the macroscale, each node corresponding to a brain region and each edge to an inter-nodal connection. Given two regions of AAL-90, they were considered structurally connected if there were at least three streamline counts ($counts \geq 3$) located between these two regions. In this way, we obtained a symmetric 90×90 connectivity matrix to represent the brain WM structural network for each subject. The workflow of the brain WM structural network construction is illustrated in Fig. 1.

Network analysis

We characterized the global topological properties of the brain WM structural networks using six parameters: network strength (S_p), global efficiency (E_{glob}), characteristic path length (L_p), clustering coefficient (C_p) and small-worldness (δ). A network is said to be small-world if $\gamma >> 1$ and $\lambda \approx 1$ or $\delta >> 1$ (Watts & Strogatz 1998). The definitions and interpretations of these topological parameters are listed in Table 2. The mean S_p is a measure of density or the total 'wiring cost' of the network. The larger of the network strength, the more expensive of the wiring cost of this network. The average shortest path length between all pairs of nodes in the network gives the L_p, which is a measure of WM connectivity integration. The average inverse shortest path length relates to the E_{glob}. If two nodes were disconnected, the path between these two disconnected nodes is assumed to have an infinite length and E_{glob} corresponds to zero (Achard & Bullmore 2007). The mean C_p for the network reflects, on average, the prevalence of clustered connectivity around individual nodes.

For the nodal topology, we focused on the nodal efficiency (E_{nod}). Its definition and interpretation can be seen in Table 2 and Rubinov & Sporns (2010).

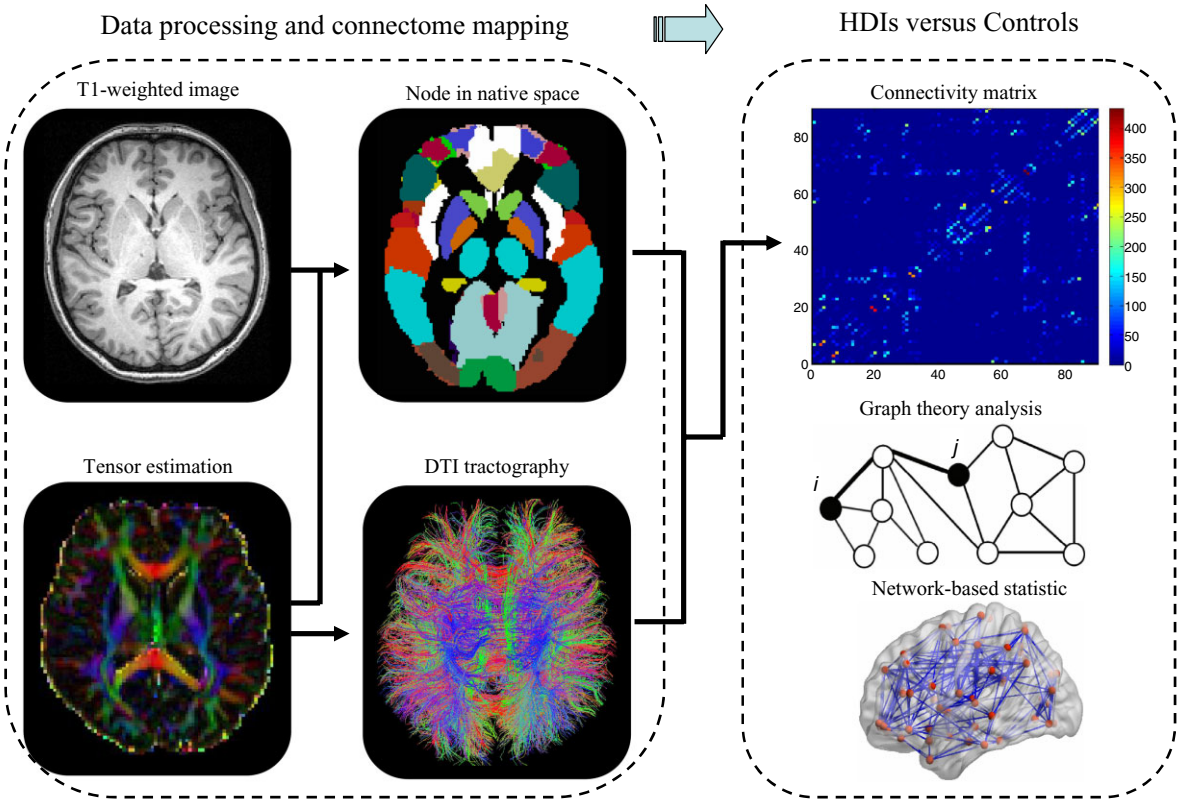

Figure 1 The workflow of constructing brain white matter (WM) structural networks for the heroin-dependent individuals (HDIs) and healthy controls (HCs) using the diffusion tensor imaging (DTI) data

Connectivity analysis

A NBS approach (Zalesky *et al.* 2012a) was used to determine the specific altered WM connections related to heroin addiction. We first used two-sample *t*-test at each edge to determine significant between-group difference in the connection. A primary component-forming threshold ($P < 0.01$, uncorrected) was applied to derive a set of suprathreshold edges. By this step, we can identify all the possible connected components or subnetworks showing altered inter-regional connectivity. The statistical significance of the size for each observed component was obtained using an empirical null distribution of maximal component sizes under the null hypothesis of random group membership (5000 permutations). The subnetworks that were significant at a level of $P < 0.05$ were reported in the current study.

Statistic analysis

Heroin addiction-related network parameters alteration

A non-parametric permutation test was used to assess the statistical significance of between-group difference in each of the global and nodal parameters. This randomization procedure was repeated 5000 times for a given network parameter and the corresponding distribution of *t*-value was obtained. We set the critical value at 95% of the distribution for each of the global and nodal parameters to test the null hypothesis. The age, gender and an age–gender interaction were entered as covariates of no interest before permutation tests.

Correlations between network parameters and clinical variables

With respect to network parameters showing significant between-group differences, we performed multiple linear regression analysis to estimate the relationship between each of the parameters and each of the clinical variables in the HDIs. The age, gender and the age–gender interaction were regressed out. The clinical variables include the age onset of addiction and the duration of addiction.

Robustness analysis

Cross-validation of the main results

Using a bootstrap approach, we estimated the confidence interval for each of the topological parameters, S_p, L_p, K_p, E_{glob}, E_{loc}, γ, δ and λ, in the HDIs and the controls. Specifically, we randomly draw an individual from the original

Table 2 The mathematical definitions and descriptions of global/nodal parameters in the current study.

Network parameters	*Definitions*	*Descriptions*
Global parameters	Network strength $S_p(G)=\sum_{i\in G} S(i)/N$	$S(i)$ is the sum of the edge weights for the node i, N is the number of nodes in the network. $S(i)$ reflects importance of the node i in the network. S_p is a measure of density or the total 'wiring cost' of the network.
	Characteristic path length $L_p=\frac{1}{1/(N(N-1))\sum_{j\neq i}1/L_{ij}}$	l_{ij} is the shortest path length between nodes i and j. Paths are sequences of distinct nodes and links in the network to represent potential routes of information flow between pairs of brain regions. The lengths of paths estimate the potential for integration between brain regions, with shorter paths implying stronger potential for integration.
	Network efficiency $E_{glob}(G)=\frac{1}{N(N-1)}\sum_{i=1}^{N}\sum_{\substack{j=1\\ j\neq i}}^{N}\frac{1}{L_{ij}}$	E_{glob} is computed on disconnected networks. Paths between disconnected nodes are defined to have infinite length and correspondingly zero efficiency.
	Clustering coefficient $C_p=\frac{1}{N}\sum_{i=1}\frac{E_i}{D_{nod}(i)(D_{nod}(i)-1)/2}$	$D_{nod}(i)$ is the degree of node i, E_i is the number of edges in the subgraph of node i and N is the number of nodes in the network. C_p reflects the prevalence of clustered connectivity around individual nodes.
Small-world parameters	Normalized clustering coefficient $\gamma=C_p^{real}/C_p^{rand}$	C_p^{real} is the clustering coefficient of the real network and C_p^{rand} is the mean clustering coefficient of 100 matched random networks.
	Normalized characteristic path length $\lambda=L_p^{real}/L_p^{rand}$	L_p^{real} is the clustering coefficient of the real network and L_p^{rand} is the mean clustering coefficient of 100 matched random networks.
	Small-worldness $\sigma=\gamma/\lambda$	A network is said to be small-world if it satisfies $\lambda\approx 1$ and $\gamma >> 1$, or $\delta=\gamma/\lambda >> 1$. Small-world organization reflects an optimal balance of functional integration and segregation.
Nodal parameter	Nodal efficiency $E_{nod}(i)=\frac{1}{N}\sum_{j\neq i}1/L_{ij}$	l_{ij} is the shortest path length between nodes i and j.

sample, put the individual back before drawing the next one and resample the subjects with replacement. Thus, each resample had the same size as the original sample. Based on the 1000 randomizations, we determined the confidence intervals for each of these parameters.

Effect of threshold in streamline counts on network parameters

Because false-positive or false-negative connections could be resulted from the selection of fibre connection threshold (Bassett *et al.* 2011; Zhang *et al.* 2014), we utilized two additional thresholds of streamline *counts* > 0 (i.e. including all non-zero entries in the connectivity matrices) and streamline *counts* ≥ 5. To this end, we constructed symmetric connectivity matrices based on AAL-90 template for each of the three different connecting thresholds (*counts* > 0, *counts* ≥ 3 and *counts* ≥ 5).

Effect of parcellation schemes on network parameters

To estimate the stability of our main findings corresponding to AAL-90 template, we repeated the network analysis by selecting the AAL-1024, a high-resolution template randomly parcellating whole brain into 1024 regions of equal volume (http://andrewzalesky.com/software.html). We selected each region in AAL-1024 template as a node and obtained a symmetric 1024 × 1024 connectivity matrix to represent the brain WM structural network for each subject.

Effect of the choice of significance level

The statistical results certainly depend on the choice of significance level. Besides of the threshold $P < 0.05$ being selected, we also adopted a much conservative threshold $P < 0.01$ to determine between-group differences in the network parameters. The aim was to test the robustness of the main results.

Head motion effects

Several recent studies (Tijssen, Jansen & Backes 2009; Kong 2014; Yendiki *et al.* 2014) demonstrated that the head motion may induce spurious group differences in DTI measures. To determine that the between-group

Table 3 Global parameters of brain WM structural networks in the heroin-dependent individuals (HDIs) and the healthy controls (HCs).

Network parameters	*Mean ± standard deviation*		P *value*	*Cohen's* d
	HDIs (n = *20)*	*HCs* (n = *18)*		
γ	3.607 ± 0.300	3.587 ± 0.706	0.9294	0.07
λ	1.214 ± 0.031	1.202 ± 0.030	0.2258	0.33
δ	2.972 ± 0.258	2.980 ± 0.581	0.9690	0.03
C_p	0.031 ± 0.004	0.032 ± 0.005	0.4002	0.08
L_p	0.018 ± 0.002	0.023 ± 0.006	1.6e-3*	1.12
E_{glob}	57.87 ± 4.998	46.27 ± 11.346	2.8e-3*	1.12
S_p	1090.6 ± 112.3	902.7 ± 183.2	6.0e-4*	1.25

The asterisk '*' indicates significant between-group difference at $P < 0.05$ (5000 permutations). Cohen's *d* indicates the value of effect size. The small, medium and large levels of the effect size are 0.2, 0.5 and 0.8, respectively, according to Cohen's definition (Cohen 1992).
γ = normalized clustering; λ = normalized path length; δ = γ/λ; C_p = cluster coefficient; L_p = characteristic path length; E_{glob} = global efficiency; S_p = network strength.

difference in network topology originated from the naïve between-group difference rather than from the head motion nuisance noise, we estimated the intra-acquisition head movement using an affine transformation approach (FSL). No significant difference was found either in any of the three displacement parameters or in any of the three rotation parameters between HDIs and controls. Even so, we still took these six head motion parameters as nuisance regressors into statistical analysis by following Yendiki *et al.* (2014).

RESULTS

Demographic and behavioural measures

Table 1 lists the demographic and behavioural measures for the HDIs. No significant between-group difference was detected in age, years of education, cigarette smoking and gender ($P > 0.05$). In the calculations, two-sample *t*-test were adopted for the age, years of education and cigarette smoking, while Fisher's exact test was adopted for the gender (SPSS, version 17.0, IBM, Armonk, NY, USA).

Network analysis

Global parameters

Table 3 lists the global parameters for both the HDIs and controls. We found that the brain WM structural networks for both groups satisfy the criteria of small-world organization, $\gamma >> 1$ and $\lambda \approx 1$, and $\delta >> 1$. Compared with the controls, the HDIs showed significantly increased E_{glob} ($P = 2.8e\text{-}3$) and S_p, ($P = 6.0e\text{-}4$), but decreased L_p ($P = 1.6e\text{-}3$). Whereas no significant between-group difference was detected in the C_p ($P = 0.4002$) and in any of small-world metrics ($P = 0.9294$ for γ, $P = 0.2258$ for λ and $P = 0.9690$ for σ).

Nodal parameter

Statistical analysis revealed uniformly significantly increased nodal efficiency in several regions in the HDIs compared with the controls ($P < 0.05$, Bonferroni's correction). According to addiction model proposed by Baler & Volkow (2006), we classified regions showing significant between-group difference into three addition-related functional systems: (1) the motivation and salience evaluation system in the orbital cortex (ORB), including the bilateral orbital superior frontal gyri (ORBsup.L/R), bilateral orbital middle frontal gyri (ORBmid.L/R), left orbital inferior frontal gyrus (ORBinf.L) and left medial orbital of superior frontal gyrus (ORBsupmed.L); (2) the cognitive control and restraining craving system in the prefrontal cortex (PFC), such as the left rectus gyrus (REC.L); and (3) the inhibition control and conflict monitoring system in the anterior cingulate gyrus (ACG), such as the left ACG. The mean values of E_{nod} and effect size (Cohen's *d*) are presented in Table 4 (Fig. 2).

Disrupted connectivity in HDIs

Using the NBS analysis, we identified a single subnetwork with significantly altered WM connections in the HDIs compared with the controls ($P < 0.05$, family-wise error corrected). This subnetwork was composed of 16 links and 17 brain regions, including the left orbital superior frontal gyrus (ORBsup.L), left insula (INS.L), left ACG, left middle frontal gyrus (MFG.L), left triangle part of inferior frontal gyrus (IFGtriang.L), bilateral rectus (REC), bilateral olfactory (OLF), bilateral supplementary motor area (SMA) and the left middle temporal gyrus (MTG.L) (Fig. 3a). Notably, all of inter-regional connections within the NBS-derived subnetwork were significantly increased in the HDIs compared with the

Table 4 Brain regions with significant difference in nodal efficiency (E_{nod}) between the heroin-dependent individuals (HDIs) and the healthy controls (HCs) (5000 permutations, $P < 0.05$, Bonferroni corrected).

Regions	*Category*	E_{nod} *(mean ± standard deviation)*		P *value*	*Cohen's* d
		HDIs (n = *20)*	*HCs* (n = *18)*		
ORBsup.L	ORB	40.86 ± 5.56	30.91 ± 8.11	2.0e-4	1.45
ORBsup.R	ORB	41.57 ± 7.07	30.12 ± 9.73	<1.0e-4	1.36
ORBmid.L	ORB	43.47 ± 5.98	31.83 ± 12.19	2.0e-4	1.23
ORBmid.R	ORB	46.73 ± 8.16	34.26 ± 12.39	<1.0e-4	1.20
ORBinf.L	ORB	59.89 ± 6.75	49.15 ± 10.68	4.0e-4	1.22
ORBsupmed.L	ORB	43.04 ± 5.40	33.88 ± 7.64	<1.0e-4	1.40
REC.L	PFC	36.46 ± 3.89	28.11 ± 6.45	<1.0e-4	1.59
ACG.L	ACG	62.42 ± 7.89	50.47 ± 9.79	2.0e-4	1.35
CAL.L	Occipital	70.36 ± 10.32	55.17 ± 15.17	4.0e-4	1.18
STG.L	Temporal	69.54 ± 8.29	55.97 ± 14.76	4.0e-4	1.15

E_{nod} was uniformly increased in the HDIs compared with the HCs.
Cohen's *d* indicates the value of effect size. The small, medium and large levels of the effect size are 0.2, 0.5 and 0.8, respectively, according to Cohen's definition (Cohen 1992).
ACG = anterior cingulate gyrus; ORB = orbital frontal cortex; PFC = prefrontal cortex.

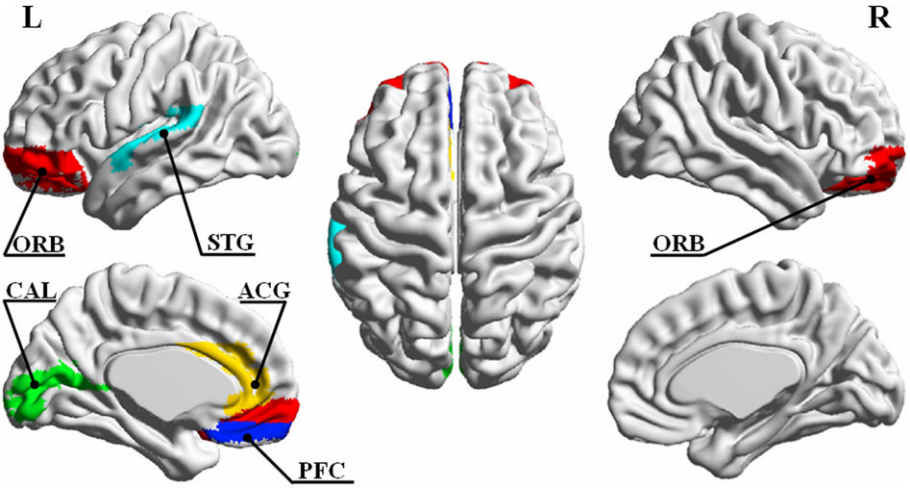

Figure 2 Rendering plot of the brain regions showing significantly increased nodal efficiency (E_{nod}) in the heroin-dependent individuals compared with the healthy controls ($P < 0.05$, Bonferroni corrected). The images were plotted with the BrainNet Viewer (http://www.nitrc.org/projects/bnv/) (Xia, Wang & He 2013). Abbreviations: ACG, anterior cingulate gyrus (yellow); CAL, calcarine cortex (green); ORB, orbital frontal cortex (red); PFC, prefrontal cortex (blue); STG, superior temporal gyrus (cyan)

controls. The detailed mean weights and *t*-values of statistic between-group comparison in the connections are listed in Supporting Information Table S4.

For each of the global parameters showing significant between-group difference (E_{glob}, S_p and L_p), we calculated its correlation with the edge weights or with the streamline counts of the NBS-derived subnetwork. Figure 3b shows that the edge weight in the subnetwork was significantly positively correlated with the S_p ($r = 0.73$, $P = 1.58e\text{-}7$) and E_{glob} ($r = 0.72$, $P = 2.91e\text{-}7$), but negatively correlated with the L_p ($r = -0.74$, $P = 1.46e\text{-}7$), across all subjects.

Correlation between network parameters and clinical variables

Neither of the inter-nodal connections of NBS-derived subnetwork nor of the significant changed topological parameters (global and nodal) was significantly correlated with the age onset of addiction or with the duration of addiction in the HDIs ($P > 0.05$).

Robustness of our findings

We first obtained the confidence interval for each of global parameters based on the AAL-90 template using

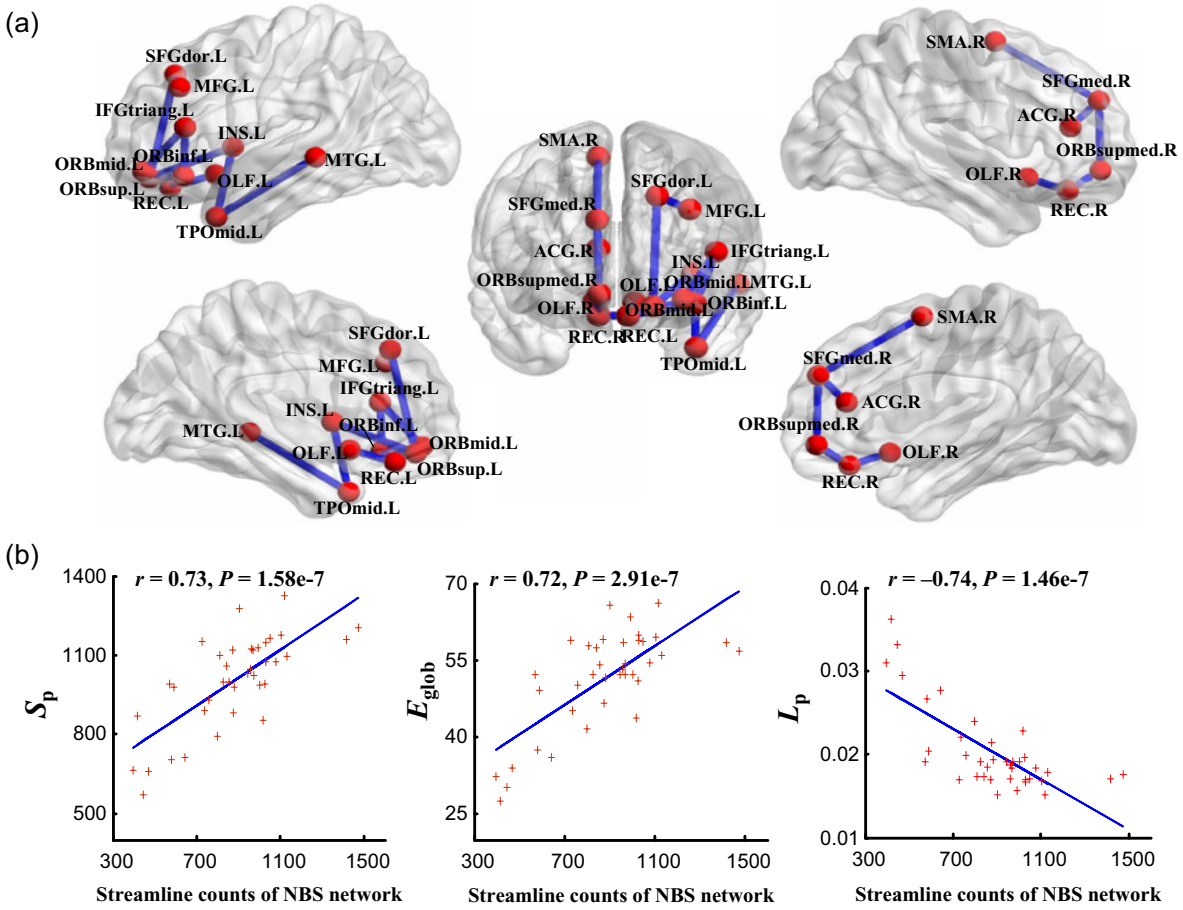

Figure 3 The subnetwork derived from the network-based statistic (NBS) analysis. (a) Increased structural connections in heroin-dependent individuals (HDIs). These connections formed a single subnetwork containing 17 nodes and 16 edges. All the 16 edges were uniformly significantly increased ($P = 0.029$, family-wise error corrected) in the HDIs compared with the controls. (b) Scatter plots of the significantly changed global parameters changing with the number of streamline counts within the NBS-derived subnetwork across all subjects. Except for the characteristic path length L_p, the other global parameters (strength S_p and global efficiency E_{glob}) were significantly positively correlated to the streamline counts within the NBS-derived subnetwork

the bootstrap approach. In the calculations, we built the distribution of global parameters across 1000 random resamples and determined the 95% confidence interval of the original sample for the HDIs and controls (Supporting Information Table S5). Then we estimated the effect of inter-regional connectivity threshold (or streamline counts) on network parameters. Statistical analysis showed that the significant level of between-group difference in topological parameters was not dependent on our selections of streamline counts ($counts > 0$ and $counts \geq 5$) as the threshold of inter-regional connectivity (Table 5). We also tested the effect of node size on the network topology using a high-resolution template, the AAL-1024 template. The change tendencies of the global parameters (S_p, E_{glob} and L_p) for the AAL-1024 template were similar to those for the AAL-90 template (Table 5). We also checked the influence of the significant levels of between-group differences on the network parameters. Compared with the controls, the HDIs showed significantly increased S_p and E_{glob}, but decreased L_p, at the threshold $P < 0.01$. Finally, the network parameters showing significant between-group difference can still be detected at $P < 0.05$ (Table 5) even though the head motion effects were regressed out.

DISCUSSION

In this study, we explored the topological organization of brain WM structural networks in HDIs. Even though both the HDIs and controls conserved small-worldness, the HDIs showed significantly increased E_{glob} and S_p, but significantly decreased L_p compared with the controls. Furthermore, the HDIs showed significantly increased nodal efficiency in the bilateral orbital frontal cortices (OFC), left PFC and left ACG compared with the controls. Moreover, based on the NBS approach, we determined a subnetwork in which the structural connectivity was significantly changed in the HDIs compared with the controls. The

Table 5 Robustness analysis to show the stability of our findings in brain topology between the heroin-dependent individuals (HDIs) and the healthy controls (HCs).

	Between-group difference in network parameters (HDIs versus HCs)						
Analysis strategy	δ	λ	γ	C_p	S_p	E_{glob}	L_p
counts > 0 in AAL-90	n.s.	n.s.	n.s.	n.s.	5.0e-4 ↑	1.5e-3 ↑	1.4e-3 ↓
counts ≥ 5 in AAL-90	n.s.	n.s.	n.s.	n.s.	4.0e-4 ↑	1.5e-3 ↑	1.4e-3 ↓
AAL-1024 template	4.2e-2 ↑	n.s.	n.s.	n.s.	9.0e-4 ↑	6.0e-4 ↑	5.0e-4 ↓
$P < 0.01$	n.s.	n.s.	n.s.	n.s.	6.0e-4 ↑	2.8e-3 ↑	1.6e-3 ↓
Head motion effects	n.s.	n.s.	n.s.	n.s.	6.6e-3 ↑	2.0e-2 ↑	1.0e-2 ↓

We listed the results obtained from selecting different brain parcellation schemes (AAL-90 and AAL-1024) and a conservative threshold ($P < 0.01$) and regressing out head motion parameters. The threshold '*counts* > 0' indicates that the two regions were connected if at least one streamline existed between a pair of brain regions. The AAL-1024 template contains 1024 regions with equal volume size.
↑ = HDIs > HCs; ↓ = HDIs < HCs; n.s. = non-significant; γ = normalized clustering; λ = normalized path length; $\delta = \gamma/\lambda$; C_p = cluster coefficient; E_{glob} = global efficiency; L_p = characteristic path length; S_p = network strength.

number of streamline counts for all WM connections in this subnetwork was significantly increased in the HDIs.

Although the brain WM structural networks for both the HDIs and the controls hold small-worldness ($\gamma >> 1$ and $\delta >> 1$, $\lambda \approx 1$), we found the HDIs showed significantly increased E_{glob}, but decreased L_p compared with the controls (Table 3). Similarly, the HDIs also showed significantly increased S_p compared with the controls. These results were consistent with a previous study (Yuan *et al.* 2010) in which the topology of brain functional network was derived from resting-state fMRI data in heroin users. As small-world properties reflect an optimal balance between local specialization and global integration (Sporns 2011), our finding of the increased global integration (increased E_{glob} and S_p, decreased L_p) and unchanged C_p in the HDIs indicate that the brain WM structural networks in HDIs may keep high wiring cost or break up the trade-off between the efficiency and cost and may shift towards a random network (Latora & Marchiori 2001).

With respect to nodal parameters, we found that the HDIs showed significantly increased E_{nod} in the bilateral OFC, left PFC and left ACG compared with the controls (Fig. 2 and Table 4). Previous studies (Kalivas & Volkow 2005; Baler & Volkow 2006) suggested that the OFC is mainly involved in motivation and salience evaluation, the PFC is responsible for craving and cognitive control and the ACG is involved in the inhibition controlling and conflict monitoring. In heroin users, the typical cognitive impairment includes poor cognitive processing, decision-making deficit, uninhibited behaviour and loss of self-control (Vassileva *et al.* 2007; Dissabandara *et al.* 2014; Yan *et al.* 2014). The disrupted WM connectivity in the PFC or in the ACG may cause impairment of cognitive control function across multiple domains, including attention, inhibition, decision and working memory, which lead to the reduced cognitive control on craving and motivation in heroin users (Ma *et al.* 2010; Moreno-Lopez *et al.* 2012; Jasinska *et al.* 2014). Notably, the NBS analysis suggested that the inter-regional connections among the paralimbic, OFC, PFC and temporal regions were significantly changed (Fig. 3a). Thus, our findings of the aberrant nodal efficiency in the bilateral OFC, left PFC and left ACG may provide evidence to some extent that heroin users have a weak cognitive control and conflict monitoring ability. When exposed to heroin-related cues, heroin users easily ignore the negative results of the addiction and turn to drug-taking behaviours (Koob & Volkow 2009).

For the changes of WM connectivity in the HDIs, their origins might be traced back to the increased number of streamlines interconnecting different gray matter nodes. Within the NBS-derived subnetwork, we detected that the number of streamline counts was significantly correlated with the changed global network metrics (L_p, S_p and E_{glob}) in the HDIs (Fig. 3b). Although we are not sure whether an increased streamline counts in this study can be ascribed to an increased number, density or coherence of axonal fibres, it is clear that the axonal fibres provides pathways for the information transferring between brain regions. The increased axonal fibres or density may imply that over-speed nerve pulses are transferred (Rushton 1951; Budd & Kisvárday 2012; Hofman 2014). The over-speed information flow may prompt HDIs to make a pat-on-the-head decision ignoring the consequences (Forstmann *et al.* 2010; Cavanagh *et al.* 2011). In addition, we found that the HDIs showed significantly increased FA and axial diffusivity ($\lambda_{//}$) in several tracts using the tract-based spatial statistic approach, including the right anterior corona radiate, right posterior limb of internal capsule, bilateral posterior thalamic radiation

and left exterior capsule (Supporting Information Fig. S1). Thus, we may infer that the increased WM connections provide a potential explanation of heroin addiction related to neuronal basis from the perspective of neural pulse transferring.

Several potential limitations exist in this study. First, the DTI data with non-isotropic voxel size and low SNR (acquired from a 1.5T MRI scanner) may bias the calculation result. To address the potential impacts of low SNR, we repeated the network analysis using different inter-regional connectivity threshold and different brain parcellation schemes and found that the results showed a high robustness across subjects (Table 5). This suggests that our findings are reliable and stable, although some suboptimal scanning parameters have been used. Second, the sources of miscalibration of hardware components may have a combined effect on fibre tracking. Gradient calibration is an important step for acquiring high-quality diffusion-weighed images and for obtaining accurate brain WM tracks (Posnansky, Kupriyanova & Shah 2011). To calibrate gradient and reduce the gradient errors, such as gradient amplitude scaling errors and background gradients, we used an affine alignment to correct the eddy current and rotated gradient direction corresponding diffusion-sensitive directions (Leemans & Jones 2009). Besides of the gradient correction, the signal dropout or the interaction between motion and field inhomogeneity should also be considered in the future study. Third, the influence of methadone on brain WM was not considered, although a previous study (Wang *et al.* 2011) suggested that the methadone treatment may affect diffusivity of brain tissues in HDIs. In this study, we analysed the correlations between the significant changed network parameters and the age onset of addiction or the duration of addiction in the HDIs. We found that the duration of addiction in the HDIs was positively correlated with S_p ($r = 0.21$, $P = 0.37$) and E_{glob} ($r = 0.22$, $P = 0.34$), but negatively with the L_p ($r = -0.21$, $P = 0.37$). Similarly, we also detected that the age onset of addiction was positively correlated with S_p ($r = 0.02$, $P = 0.93$) and E_{glob} ($r = 0.02$, $P = 0.93$), but negatively with L_p ($r = -0.04$, $P = 0.86$). However, none of these correlations reached the significant level ($P < 0.05$). To uncover the brain WM structural network alteration in HDIs, we should collect more detailed clinical variables and consider the effect of methadone on the topology of brain networks in the future study. Finally, as this is a cross-sectional study, we cannot make sure whether the topological differences are a consequence of heroin exposure or they existed before addiction and served as predisposing factors to the development of addiction. Genetic and longitudinal imaging studies are required to resolve this issue.

CONCLUSION

In summary, we constructed brain WM structural networks, analysed the topological properties according to graph theory and detected abnormal axonal fibre connectivity and topological organization in the HDIs. The HDIs showed increased global integration (increased E_{glob} and S_p, decreased L_p) along with increased nodal efficiency in the bilateral OFC, left PFC and left ACG. We also detected increased WM connections in the OFC, PFC and ACG in the HDIs. These results may suggest the disruption of brain WM structural network in heroin-dependent users.

Acknowledgements

This work was partially supported by the Guangdong No. 2 Provincial People's Hospital, the funding of National Natural Science Foundation of China (Grant numbers: 81271548, 81371535, 81428013, 81471654 and 81471639) and the Science and Technology Planning Project of Guangdong Province, China (Grant numbers: 2011B031800044, 2012A030400019 and 2013B021800172). We also thank the three anonymous reviewers for their constructive suggestions and thanks to all individuals who served as the research participants.

Authors Contribution

RZ, GJ, JT and RH designed the study. RZ and GJ undertook the data analyses. YQ, XM, SL and TW collected the clinical and MRI data. XW, AZ, ML, JW and CL contributed to the data analyses. RZ and RH wrote the manuscript. All authors contributed to and approved the final manuscript.

References

Achard S, Bullmore E (2007) Efficiency and cost of economical brain functional networks. PLoS Comput Biol 3:e17.

Baler RD, Volkow ND (2006) Drug addiction: the neurobiology of disrupted self-control. Trends Mol Med 12:559–566.

Bassett DS, Brown JA, Deshpande V, Carlson JM, Grafton ST (2011) Conserved and variable architecture of human white matter connectivity. Neuroimage 54:1262–1279.

Budd JM, Kisvárday ZF (2012) Communication and wiring in the cortical connectome. Front Neuroanat 6:42. doi: 10.3389/fnana. 2012.00042

Cavanagh JF, Wiecki TV, Cohen MX, Figueroa CM, Samanta J, Sherman SJ, Frank MJ (2011) Subthalamic nucleus stimulation reverses mediofrontal influence over decision threshold. Nat Neurosci 14:1462–1467.

Cohen J (1992) A power primer. Psychol Bull 112:155–159.

Dissabandara LO, Loxton NJ, Dias SR, Dodd PR, Daglish M, Stadlin A (2014) Dependent heroin use and associated risky behaviour: the role of rash impulsiveness and reward sensitivity. Addict Behav 39:71–76.

Fornito A, Zalesky A, Pantelis C, Bullmore ET (2012) Schizophrenia, neuroimaging and connectomics. Neuroimage 62:2296–2314.

Forstmann BU, Anwander A, Schäfer A, Neumann J, Brown S, Wagenmakers E-J, Bogacz R, Turner R (2010) Cortico-striatal connections predict control over speed and accuracy in perceptual decision making. Proc Natl Acad Sci U S A 107: 15916–15920.

Goldstein RZ, Volkow ND (2011) Dysfunction of the prefrontal cortex in addiction: neuroimaging findings and clinical implications. Nat Rev Neurosci 12:652–669.

Griffa A, Baumann PS, Thiran J-P, Hagmann P (2013) Structural connectomics in brain diseases. Neuroimage 80:515–526.

Hagmann P, Cammoun L, Gigandet X, Gerhard S, Ellen Grant P, Wedeen V, Meuli R, Thiran J-P, Honey CJ, Sporns O (2010) MR connectomics: principles and challenges. J Neurosci Methods 194:34–45.

He Y, Evans A (2014) Magnetic resonance imaging of healthy and diseased brain networks. Front Hum Neurosci 8:890.

Hofman MA (2014) Evolution of the human brain: when bigger is better. Front Neuroanat 8:15. doi: 10.3389/fnana.2014.00015

Holmes D (2012) Prescription drug addiction: the treatment challenge. Lancet 379:17–18.

Jasinska AJ, Stein EA, Kaiser J, Naumer MJ, Yalachkov Y (2014) Factors modulating neural reactivity to drug cues in addiction: a survey of human neuroimaging studies. Neurosci Biobehav Rev 38:1–16.

Jiang G, Wen X, Qiu Y, Zhang R, Wang J, Li M, Ma X, Tian J, Huang R (2013) Disrupted topological organization in whole-brain functional networks of heroin-dependent individuals: a resting-state fMRI study. PLoS ONE 8:e82715.

Kalivas PW, Volkow ND (2005) The neural basis of addiction: a pathology of motivation and choice. Am J Psychiatry 162:1403–1413.

Kim D-J, Skosnik PD, Cheng H, Pruce BJ, Brumbaugh MS, Vollmer JM, Hetrick WP, O'Donnell BF, Sporns O, Puce A (2011) Structural network topology revealed by white matter tractography in cannabis users: a graph theoretical analysis. Brain Connect 1:473–483.

Kong X-Z (2014) Association between in-scanner head motion with cerebral white matter microstructure: a multiband diffusion-weighted MRI study. PeerJ 2:e366.

Koob GF (2002) Neurobiology of drug addiction. In: Kandel DB, ed. Stages and Pathways of Drug Involvement: Examining the Gateway Hypothesis, pp. 337–361. New York, NY: Cambridge University Press.

Koob GF, Volkow ND (2009) Neurocircuitry of addiction. Neuropsychopharmacology 35:217–238.

Latora V, Marchiori M (2001) Efficient behavior of small-world networks. Phys Rev Lett 87:198701.

Leemans A, Jones DK (2009) The B-matrix must be rotated when correcting for subject motion in DTI data. Magn Reson Med 61:1336–1349.

Levran O, Londono D, O'hara K, Nielsen D, Peles E, Rotrosen J, Casadonte P, Linzy S, Randesi M, Ott J (2008) Genetic susceptibility to heroin addiction: a candidate gene association study. Genes Brain Behav 7:720–729.

Li Q, Wang Y, Zhang Y, Li W, Yang W, Zhu J, Wu N, Chang H, Zheng Y, Qin W, Zhao L, Yuan K, Liu J, Wang W, Tian J (2012) Craving correlates with mesolimbic responses to heroin-related cues in short-term abstinence from heroin: an event-related fMRI study. Brain Res 1469:63–72.

Li W, Li Q, Zhu J, Qin Y, Zheng Y, Chang H, Zhang D, Wang H, Wang L, Wang Y, Wang W (2013) White matter impairment in chronic heroin dependence: a quantitative DTI study. Brain Res 1531:58–64.

Liu J, Liang J, Qin W, Tian J, Yuan K, Bai L, Zhang Y, Wang W, Wang Y, Li Q (2009) Dysfunctional connectivity patterns in chronic heroin users: an fMRI study. Neurosci Lett 460:72–77.

Ma N, Liu Y, Li N, Wang C-X, Zhang H, Jiang X-F, Xu H-S, Fu X-M, Hu X, Zhang D-R (2010) Addiction related alteration in resting-state brain connectivity. Neuroimage 49:738–744.

Moreno-Lopez L, Stamatakis EA, Fernandez-Serrano MJ, Gomez-Rio M, Rodriguez-Fernandez A, Perez-Garcia M, Verdejo-Garcia A (2012) Neural correlates of hot and cold executive functions in polysubstance addiction: association between neuropsychological performance and resting brain metabolism as measured by positron emission tomography. Psychiatry Res 203:214–221.

Mori S, Zhang J (2006) Principles of diffusion tensor imaging and its applications to basic neuroscience research. Neuron 51:527–539.

Posnansky O, Kupriyanova Y, Shah NJ (2011) On the problem of gradient calibration in diffusion weighted imaging. Int J Imag Syst Tech 21:271–279.

Rubinov M, Sporns O (2010) Complex network measures of brain connectivity: uses and interpretations. Neuroimage 52:1059–1069.

Rushton WA (1951) A theory of the effects of fibre size in medullated nerve. J Physiol 115:101–122.

Schmidt A, Walter M, Gerber H, Schmid O, Smieskova R, Bendfeldt K, Wiesbeck GA, Riecher-Rossler A, Lang UE, Rubia K, McGuire P, Borgwardt S (2013) Inferior frontal cortex modulation with an acute dose of heroin during cognitive control. Neuropsychopharmacology 38:2231–2239.

Sporns O (2011) The human connectome: a complex network. Ann N Y Acad Sci 1224:109–125.

Tang YL, Zhao D, Zhao C, Cubells JF (2006) Opiate addiction in China: current situation and treatments. Addiction 101:657–665.

Tijssen R, Jansen JF, Backes WH (2009) Assessing and minimizing the effects of noise and motion in clinical DTI at 3T. Hum Brain Mapp 30:2641–2655.

Vassileva J, Petkova P, Georgiev S, Martin EM, Tersiyski R, Raycheva M, Velinov V, Marinov P (2007) Impaired decision-making in psychopathic heroin addicts. Drug Alcohol Depend 86:287–289.

Volkow ND, Li T-K (2004) Drug addiction: the neurobiology of behaviour gone awry. Nat Rev Neurosci 5:963–970.

Volkow ND, Wang G-J, Fowler JS, Tomasi D, Baler R (2013) Neuroimaging of addiction. In: Seeman P, Madras B eds. Imaging of the Human Brain in Health and Disease, 1st edn, pp. 1–26. Oxford: Elsevier Int.

Walter M, Denier N, Gerber H, Schmid O, Lanz C, Brenneisen R, Riecher-Rossler A, Wiesbeck GA, Scheffler K, Seifritz E, McGuire P, Fusar-Poli P, Borgwardt S (2014) Orbitofrontal response to drug-related stimuli after heroin administration. Addict Biol. doi: 10.1111/adb.12145. [Epub ahead of print].

Wang Y, Li W, Li Q, Yang W, Zhu J, Wang W (2011) White matter impairment in heroin addicts undergoing methadone maintenance treatment and prolonged abstinence: a preliminary DTI study. Neurosci Lett 494:49–53.

Watts DJ, Strogatz SH (1998) Collective dynamics of 'small-world' networks. Nature 393:440–442.

Xia M, Wang J, He Y (2013) BrainNet Viewer: a network visualization tool for human brain connectomics. PLoS ONE 8:e68910.

Xiao Z, Lee T, Zhang JX, Wu Q, Wu R, Weng X, Hu X (2006) Thirsty heroin addicts show different fMRI activations when

exposed to water-related and drug-related cues. Drug Alcohol Depend 83:157–162.

Yan W-S, Li Y-H, Xiao L, Zhu N, Bechara A, Sui N (2014) Working memory and affective decision-making in addiction: a neurocognitive comparison between heroin addicts, pathological gamblers and healthy controls. Drug Alcohol Depend 134:194–200.

Yendiki A, Koldewyn K, Kakunoori S, Kanwisher N, Fischl B (2014) Spurious group differences due to head motion in a diffusion MRI study. Neuroimage 88:79–90.

Yuan K, Qin W, Liu J, Guo Q, Dong M, Sun J, Zhang Y, Liu P, Wang W, Wang Y (2010) Altered small-world brain functional networks and duration of heroin use in male abstinent heroin-dependent individuals. Neurosci Lett 477:37–42.

Zalesky A, Cocchi L, Fornito A, Murray MM, Bullmore E (2012a) Connectivity differences in brain networks. Neuroimage 60:1055–1062.

Zalesky A, Solowij N, Yücel M, Lubman DI, Takagi M, Harding IH, Lorenzetti V, Wang R, Searle K, Pantelis C (2012b) Effect of long-term cannabis use on axonal fibre connectivity. Brain 135:2245–2255.

Zhang R, Wei Q, Kang Z, Zalesky A, Li M, Xu Y, Li L, Wang J, Zheng L, Wang B (2014) Disrupted brain anatomical connectivity in medication-naïve patients with first-episode schizophrenia. Brain Struct Funct. doi: 10.1007/s00429-014-0706-z. [Epub ahead of print].

SUPPORTING INFORMATION

Additional Supporting Information may be found in the online version of this article at the publisher's web-site:

Appendix S1 Data aquisition.

Figure S1 Brain white matter with the significant altered diffusion metrics in the heroin-dependent individuals (HDIs) compared with the healthy controls. (a) Fractional anisotropy (FA); (b) Axial diffusivity ($\lambda_{//}$); (c) overlap brain white matter tracts derived from both FA and $\lambda_{//}$ analyses, coloured by blue.

Table S1 Summary of diffusion magnetic resonance imaging studies about heroin-dependent individuals (HDIs) compared with healthy controls (HCs).

Table S2 The detailed clinical description for each heroin-dependent individual (HDIs).

Table S3 Names and abbreviations of the regions of interest (ROIs) defined in the AAL-90 template (45 regions for each hemisphere).

Table S4 Inter-nodal connections with significant difference between the heroin-dependent individuals (HDIs) and the healthy controls (HCs) derived from the network-based statistic (NBS) analysis. Compared with the controls, the HDIs showed significantly increased streamline counts in each of the inter-nodal connections ($P = 0.029$, FWE correction).

Table S5 Confidence interval of global parameters in the brain networks of the heroin-dependent individuals (HDIs) and the healthy controls (HCs).

